Proceedings of IMECE 2004:
2004 ASME International Mechanical Engineering Congress and RD&D Expo
November 15-21, Anaheim, CA

IMECE2004-61334

MICRO-PNEUMATIC LOGIC

Albert K. Henning
Director of Technology
Redwood Microsystems, Inc.
959 Hamilton Avenue
Menlo Park, CA 94025
650 617 0854
henning@redwoodmicro.com

ABSTRACT

Advances in silicon membrane and microvalve technology continue to be made. Microvalves utilizing membranes have always encompassed the attribute of an on-off switch, thereby suggesting a logic element, although their main application has been arguably as a proportional flow control device.

Recently, an analogy has been suggested between a microelectronic, *p*-channel MOSFET, and a microvalve. The analogy includes a qualitative comparison between the flow vs. pressure relationship for the microvalve, and the current vs. voltage relationship for the MOSFET. It also includes a simple, small-signal frequency analysis of microvalve flow, based on a 'saturation' flow behavior chosen arbitrarily to be similar to that in a MOSFET.

In this work, a quantitative and rigorous model for the flow vs. pressure relationship for a microvalve is presented. The model couples the mechanical behavior of a silicon membrane, with the fluid mechanical behavior facilitated by the membrane's motion. The model is substantiated by measurements. The model is compared by analogy to the related MOSFET model equations. The pneumatic model is then applied to both a normally-closed microvalve, and a normally-closed poppet valve. The normally-closed microvalve is analogous to a *p*-MOSFET. The normally-closed poppet microvalve is analogous to an *n*-MOSFET. By appropriate physical coupling of these two devices, a fully complementary pneumatic NOR gate results. The quantitative pneumatic flow model is applied to this structure, and the logic transfer function is obtained. The ramifications of the results for scaled, micro-pneumatic logic devices will be discussed.

INTRODUCTION

A qualitative analogy between electronic MOSFETs and pneumatic microvalves has recently been suggested [1]. The analogy began with a lateral silicon microvalve structure, similar to that reported in earlier work [2]. The position of the membrane relative to the lateral valve seat was controlled by a pneumatic signal. The structure was stated to be analogous to a *p*-MOSFET. Measurements of flow vs. outlet, control, and inlet pressures were taken. Qualitative observations of linear and saturation behavior were made. The effect of a threshold pressure, analogous to the threshold voltage in a MOSFET, was noted.

An extension of this work presented a saturation flow equation for this same microvalve structure [3]. The flow equation was chosen arbitrarily to match the form of the saturation current equation for a MOSFET. Two signal inversion structures (that is, NOR gates, or inverters) were proposed, based on the *p*-MOSFET-like microvalve. One structure utilized an 'enhancement-mode' microvalve as a load device, while the other utilized a 'depletion-mode' microvalve. Steady-state and small-signal flow measurements in these two structures were made.

These devices represent by no means the first attempts at pneumatic logic based on compressible gas flow. During the 1960's, before microelectronics came to the forefront of computing and control technology, pneumatic logic structures were devised and deployed, for instance in the propulsion and manipulation of punch cards in early computing systems [6]. Pneumatic microvalves are also not new [5, 7, 8], although their application to date has been more toward traditional analog control, or for gas (pneumatic) control of liquid (hydraulic) flow, and not for realization of digital logic.

The burgeoning field of microfluidics has attracted much attention in the last decade, and it is worth a moment to discuss logic structures in this context. The term 'microfluidics' is usually taken to encompass the control and distribution of biologically-significant, incompressible liquids. As such, logic structures working according to microfluidic principles might more generally be called microhydraulic logic devices, as opposed to micropneumatic logic devices.

One of the earlier hydraulic logic devices was reported in 1954 [4]. A fluidic input to the gate resulted in a fluidic output. A millimeter-sized device exhibited gate switching frequencies of 30 Hz. Other early efforts have also been reported [10].

In the last decade, several approaches have emerged regarding the performance of logic operations using microfluidic circuits. In one instance, a concept for a hydraulic ring oscillator was devised [9]. In another instance, devices based on microelectrochemical behavior have been reported [11]. In these logic structures, the electrochemical response of fluid in a microchannel to a voltage signal results in either an electrical or an optical output, depending upon the nature of the working fluid.

Digital microfluidics based on electrowetting [12, 13] have received recent attention. In these devices, electrical signals are used to modulate the contact angle between a liquid and a control *surface*. That is, the enclosed channel usually used to guide compressible or incompressible microflow is absent. Modulation of the contact angle is evidence of a change in surface tension. This surface tension change provides the motive force to impel liquid drops and streams across the control surface.

Highly integrated microfluidic arrays with closed channels have been developed [14]. These arrays are stated to be based on membranes actuated hydraulically, although nothing precludes pneumatic actuation. The actuation of the membranes is effected through control lines, which are distinct from the flow channels in which the biologically significant liquids move. As such, the arrangement affords a reduction in system complexity, by utilizing digitally multiplexed control lines. However, hydraulic logic is not, strictly speaking, employed: the readout of the array is stated to be optical, and not fluidic, in nature.

Most recently, microhydraulic logic structures were conceived and constructed [15]. In this instance, NOT, AND, OR, XOR, NAND, and NOR gates were constructed. Flow color represented a logical '0' or '1' state. State changes were effected using nonlinearities in flow difference between channels. The nonlinearities were created by using an external mechanical stylus to modulate the flow resistance of individual channels. As with the previous example, while the logical inputs were fluidic, the outputs were optical (changes in fluid color).

More complicated microvalve structures have been created, with both analog and digital control in mind [16]. In this instance, the actuation method of the valve gate is unspecified, although pneumatic actuation is not precluded.

As mentioned earlier, neither the notion of a pneumatic logic element [6], nor the flow vs. pressure behavior of a pneumatic microvalve [7], is new. Nonetheless, the extension of the MOSFET-microvalve analogy (to encompass a pneumatic logic element in microvalve form), and the exciting prospects for such elements (for instance, to facilitate micro compressible flow arrays, or microfluidic arrays, or to enable non-electronic computation in environments hazardous to electronics), mean that the initial analogy of [1, 3] deserves substantial further investigation. It is the main purpose of this work to carry out that investigation.

Toward that end, the equations relating compressible gas flow to the pneumatic inputs for a pneumatically actuated microvalve will be presented. Measurements substantiating the flow model, and the pneumatic actuation model, will be given.

From the model equations, the 'linear' and 'saturation' characteristics of compressible flow in microvalves will be immediately clear, as manifestations of subsonic and sonic flow.

After completing this quantitative description of compressible gas flow in microvalves, the overall pneumatic model will be applied to two types of microvalves: a vertical, normally-closed microvalve, analogous to a *p*-MOSFET; and a vertical, normally-closed poppet microvalve, analogous to a *n*-MOSFET.

Using these two microvalve structures, a novel, fully complementary, micropneumatic logic element is proposed. Again using the pneumatic, compressible gas flow models for the system, the transfer characteristic for a representative micropneumatic logic NOR gate will be derived.

The work will conclude with a discussion, including the implications of this work for transient response of micropneumatic logic gates, and for the effect on transition time of scaling the gate size to smaller dimensions.

MICROVALVE FLOW MODEL

Figure 1 portrays two instances of a normally-open microvalve. The upper portion of the figure is a lateral microvalve, after [2] and [1]. The distance z is the gap between the membrane and the valve seat, which has primary control over the flow. In this structure, the membrane shape is equally dependent upon both P_i and P_o. Flow moves laterally, from high pressure to low, P_i to P_o.

The lower portion of the figure is a vertical microvalve, which is commonly used [18]. In this instance, however, the transmembrane pressure, which controls the position of the membrane relative to the valve seat, is primarily dependent only upon P_o. The effect of P_i is limited by the ratio of the membrane area impinged by P_i, versus that impinged by P_o. For small such area ratios, most of the complications associated with inhomogeneous membrane pressure loading disappear, and later analysis is simplified. The width of the valve seat is small relative to the membrane area. By analogy, this structure is akin to an 'edgeless' MOSFET. Unlike the lateral microvalve structure, there are no edges to the valve seat, and so no leakage paths where the membrane may not contact the valve seat tightly. Flow moves vertically, from high pressure to low, P_i to P_o.

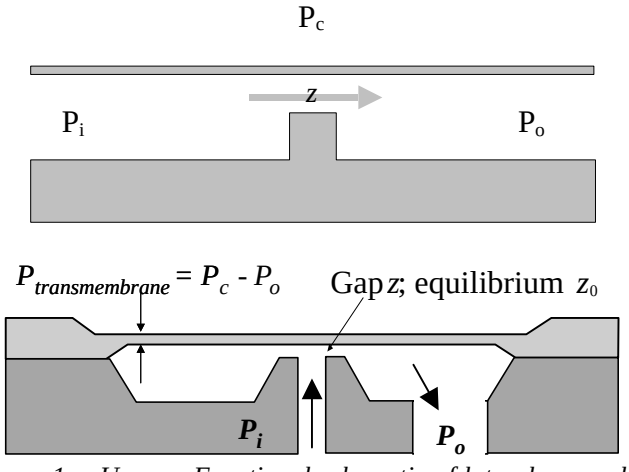

Figure 1: Upper: Functional schematic of lateral, normally-open pneumatic microvalve, after [1]. Lower: Actual schematic of typical vertical, normally-open microvalve.

The vertical microvalve has a flexible membrane, whose position z relative to the valve seat is controlled by the difference between pressure P_c, and the inlet and outlet pressures P_i and P_o. The gap $z = z_0 - s$ is essential to the control of flow. Equation (1) quantifies the change in membrane position s from its neutral position [20]. The membrane thickness is h, the area is a, and the Young's modulus is E. The coefficients A_s and B_s are dimensionless functions of a and h, as well as of Poisson's ratio for the membrane material.

$$\frac{(P_c - P_o)a^4}{Eh^4} = A_s \frac{s}{h} + B_s \frac{s^3}{h^3} \tag{1}$$

For small membrane deflections, the third-order term in Equation (1) can be ignored leaving:

$$\frac{P_{co}a^4}{Eh^4} \cong A_s \frac{s}{h} \tag{2}$$

From Equation (2), the threshold condition can be observed immediately:

$$P_t \equiv EA_s \frac{h^3 z_0}{a^4} \tag{3}$$

Equation (3) shows that the threshold transmembrane pressure is related to the initial gap, the membrane size parameters, and the membrane mechanical properties as specified by Young's modulus and Poisson's ratio. Note that, because it is a differential pressure, the threshold pressure can be negative. Also, the initial gap z_0 can be negative, as well. A negative value of z_0 corresponds to a normally-closed valve, while a positive value corresponds to normally-open valve.

The flow through the microvalve is governed by the effective area of the microvalve. A full accounting for this effective area has been given elsewhere [18, 19]. Equation (4) shows a simplification of the effective area which may be applied to the microvalves analyzed here. In this expression, W is the perimeter length of the valve seat. In the latter portion of Equation (4), the expressions for the threshold pressure, and the control-to-outlet differential transmembrane pressure, from Equations (3) and (2), have been substituted.

$$A_{eff} = Wz = W(z_0 - s) = Wa\frac{a^3}{h^3}\frac{1}{A_s E}(P_t - P_{co}) \tag{4}$$

Using Equation (4), the overall compressible gas flow model, covering both sonic and subsonic regions of the compressible flow, can be written, as in Equations (5) [18, 19].

$$\dot{m}_{sonic} = C_d C_v \frac{a(g)}{\sqrt{RT}} Wa \frac{a^3}{h^3}\frac{1}{A_s E}(P_t - P_{co})P_i \tag{5}$$

$$\dot{m}_{subsonic} = C_d C_v \frac{d(g)}{\sqrt{RT}} Wa \frac{a^3}{h^3}\frac{1}{A_s E}(P_t - P_{co})P_i \left(\frac{P_o}{P_i}\right)^{\frac{g+1}{2g}} \sqrt{\left(\frac{P_i}{P_o}\right)^{\frac{g-1}{g}} - 1}$$

In the microvalve flow model in Equations (5), g is the specific heat ratio for the compressible gas. d and a are the usual functions of g. R is the universal gas constant, divided by the gas molecular weight. T is the stagnant gas temperature as the gas enters the valve. C_d is the coefficient of discharge for the effective orifice created by the valve inlet and the membrane, while C_v is the coefficient of flow, which accounts for non-zero flow resistances which may develop as the compressible gas transits the entire valve structure. Typically, both C_d and C_v have values close to unity.

The work in Refs. [18] and [19] described the full behavior of microvalve flow, under sonic and subsonic conditions. Sonic flow develops when the gas velocity reaches the speed of sound. This condition is achieved when the ratio of the inlet pressure to the outlet pressure exceeds a critical factor. For most atmospheric gases, such as air, nitrogen, and oxygen, this factor is very close to 2.

The earlier work also accounted for the additional non-linearities of flow as the valve first opens. Because of the approximation employed, note that Equations (5) do not account for the cubic dependence of s on transmembrane pressure, for large ($s > h$) deflections, nor for the full transition to orifice-controlled flow [22].

It is worth comparing Equations (5) to the linear and saturation equations for drain-to-source current flow in a short-channel MOSFET. These are given in Equations (6). Some quantitative analogies are immediately apparent. For instance, the electronic gate and threshold voltages map directly to the control and threshold pressures. And, the drain voltage maps, more or less, to the inlet pressure. Note in particular the linear dependence of the saturation current on drain voltage. This dependence is mimicked in the sonic flow equation by the linear dependence on the inlet pressure. However, other physical analogies are less obvious. Only the full microvalve flow equations, which incorporate the non-linearities of the membrane deflection and effective area, and more sophisticated MOSFET current equations, can clarify the situation. It will remain for a subsequent work to compare and contrast the MOSFET current equations with the micropneumatic valve flow equations.

$$I_{DS,linear} = \frac{W}{L} m_n C'_{ox}\left[V_G - V_T - \frac{V_D}{2}\right]V_D$$

$$I_{DS,sat} = \frac{1}{2}\frac{W}{L} m_n C'_{ox}\left[V_G - V_T\right]^2(1 + lV_D) \tag{6}$$

MEASUREMENTS OF MICROVALVES

We now turn our attention to measurements of microvalve behavior, which substantiate the pneumatic actuation and flow model.

Figure 2a shows the measured and modeled deflection of a silicon membrane under pneumatic actuation. The model equation is Equation (1). The derived coefficients for A_s and B_s are 74.5 and 38.9, respectively. These values are close to the theoretically predicted values of 66.2 and 31.1, for a silicon membrane which is 50 μm thick, and 4.5 mm square. The differences between the measured and predicted coefficient values are ascribed to details of the membrane fabrication. In particular, the measured membrane has a central boss, whereas Equation (1) presumes a boss-free membrane. Also, the membrane as fabricated has a radius of curvature at its attachment point to the membrane frame, equal to 15 μm. ANSYS simulations show this radius of curvature is enough to

account for the difference between the observed and predicted values of the coefficients, even without a central membrane boss.

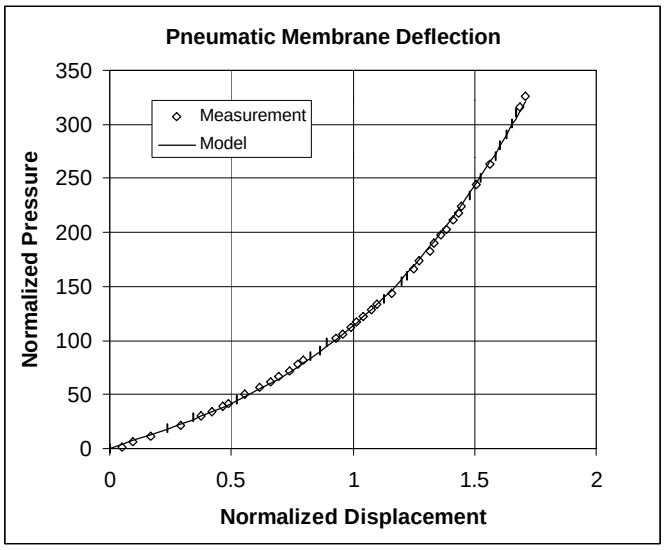

Figure 2: Measured and modeled displacement vs. pressure for a silicon membrane. The membrane thickness is 50 µm. The square membrane area is 4.5 mm. The pressure is the transmembrane pressure.

Figure 3 shows measured and modeled flow vs. gap for a microvalve constructed using the membrane of Figure 2. In this figure, the full flow model from Ref. [18] is employed. To the degree that the valve gap *z* is related linearly to the control pressure as in Equation (1), the flow curves can be compared by analogy to the typical MOSFET current vs. gate voltage characteristic. The microvalve flow is seen to level off once the membrane is separated by a distance which is approximate 25% of the inlet diameter. This transition – from seat-controlled flow, to orifice-controlled flow [22] – is compared most appropriately to current in a MOSFET, when the gate voltage becomes so large that incremental increases in the vertical channel electric field, caused by the gate voltage, produce no additional depth in the transistor inversion layer, due to screening by the channel carriers.

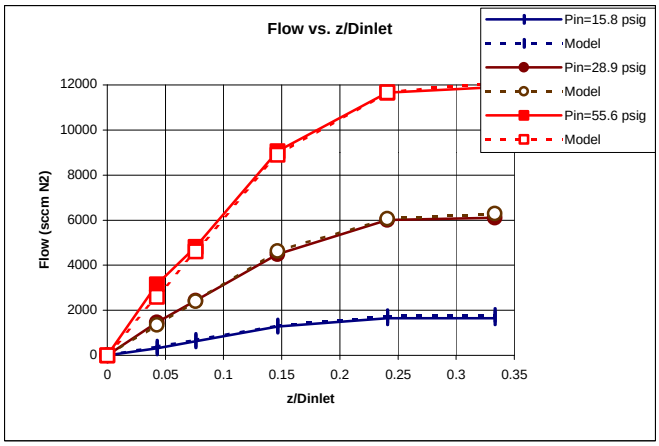

Figure 3: Microvalve flow vs. gap (measured and modeled). 'z=0' means P_{co} equals the threshold pressure P_t.

Figure 4 shows measured and modeled flow vs. inlet pressure for the same microvalve of Figure 3. These curves are analogous to the current vs. drain voltage curves for a short-channel MOSFET. As with Figure 3, the effect of the membrane control pressure occurs through the parameter *z*, the gap between the membrane and the valve seat.

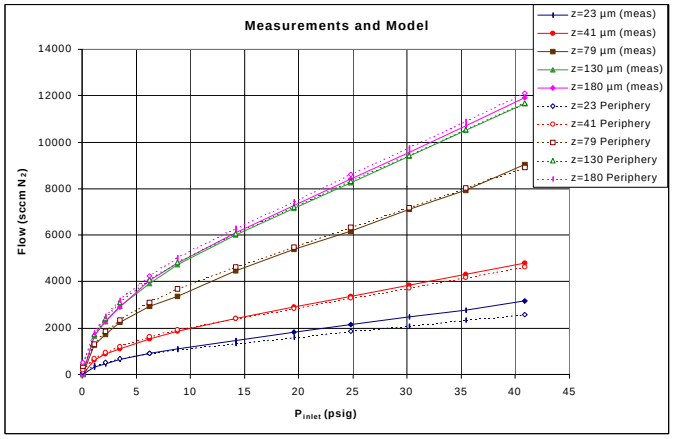

Figure 4: Microvalve flow vs. pressure (measured vs. model). The inlet structure is square, with D_{inlet} = 540 µm. The membrane parameters are as in Figures 2 and 3. After Ref. [18].

PNEUMATIC MICROVALVES FOR MICROPNEUMATIC LOGIC

Using the model and measurements from the previous section as a basis, we can now construct the microvalves required to create micropneumatic logic devices. Figure 5 shows a cross-section schematic of a normally-closed poppet microvalve, whose behavior is analogous to the normally-off *n*-channel MOSFET. Note that the microvalve is constructed so that, when the control pressure equals the outlet pressure, the built-in tension in the mechanically-offset membrane maintains the valve in an 'off' condition. Only when the control pressure exceeds the outlet pressure by an amount sufficient to overcome this built-in offset, does the microvalve open and enable gas to flow. The built-in tension, or mechanical offset, is thus directly and physically responsible for the threshold pressure condition of Equation 3.

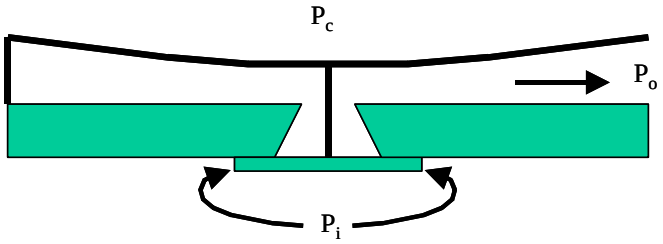

Figure 5: Cross-section of a normally-closed poppet microvalve. Flow directions are indicated by the arrows.

Keeping this figure in mind, the pneumatic actuation and flow model can be utilized to predict the flow vs. pressure characteristics of this normally-closed poppet microvalve. Figures 6 and 7 present modeling results for such a microvalve. The physical dimensions and properties are as follows: silicon is the microvalve material; the inlet dimension is 85 µm; the membrane thickness is 50 µm; the square membrane side is 4.5

mm; and the initial gap is –4 μm (a negative number indicating the initial tension, or mechanical offset, in the membrane).

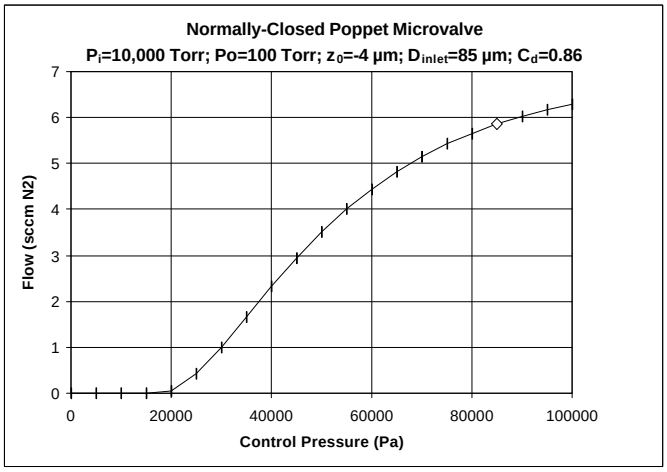

Figure 6: Control pressure characteristic for a normally-closed poppet microvalve. The gas is nitrogen, and the gas stagnant temperature is 298 K.

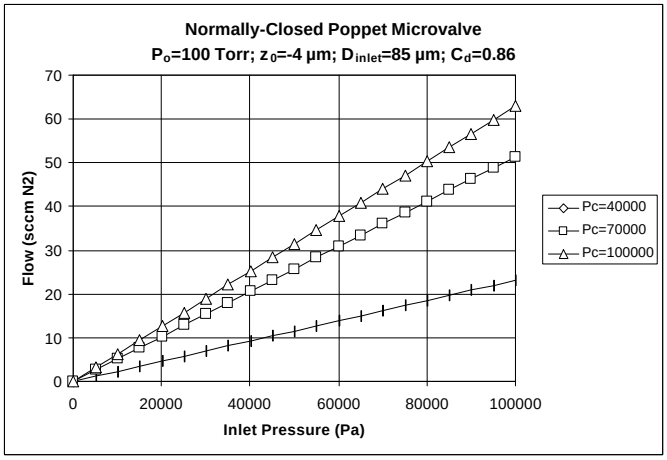

Figure 7: Inlet pressure characteristic for the normally-closed poppet microvalve of Figure 6.

Figure 8 shows a cross-section of a normally-closed microvalve. As should be clear from the figure, and the relative positions of control and outlet pressures, this device is analogous to a *p*-MOSFET, because the control pressure referenced to the outlet pressure must be negative, in order for the microvalve to enable flow. Also, as with Figure 5, note that Figure 8 indicates the microvalve in the 'off' position. The initial tension in the membrane, due to the mechanical offset built-in during the construction of the microvalve, ensures that the threshold pressure is negative, per Equations (1) and (3). That is: an initial gap z_0 of –4 μm, results in a requirement that P_{co} be *less than* the absolute value of the threshold pressure, in order for gas to flow.

The flow curves for this normally-closed, *p*-MOSFET-like microvalve, will not be presented, as from a model perspective they are identical to those of Figures 6 and 7, with the signs of flow and pressure inverted.

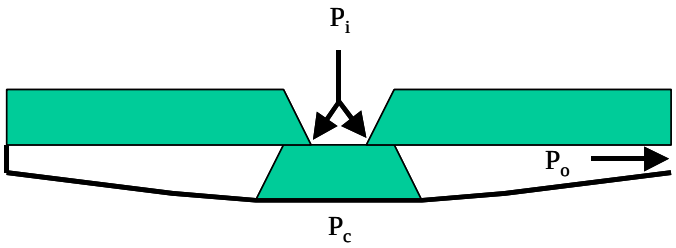

Figure 8: Cross-section of a normally-closed microvalve.

LOGICAL INVERTER CREATED FROM PNEUMATIC MICROVALVES

Using the two complementary microvalve structures from the preceding section, a logical NOR gate, or inverter, is constructed quickly.

Figure 9 shows two such micropneumatic logic gates, cascaded one after the other. The upper valves in each logic stage are normally-closed microvalves, while the lower valves are normally-closed poppet microvalves. The highest and lowest pressures in the system are indicated by PHI and PLO. These pressures are analogous to VDD and VSS in a CMOS inverter structure. High pressures are indicated with cross-hatching in Figure 9.

Two inverters are shown cascaded, so as to illustrate at once the two logical states afforded by this construction. In order to understand the operation, consider that a logic signal (a pressure field) arrives at the left-hand stage, so that PIN is set high, and POUT is set low. This state opens the poppet microvalve, and maintains closure in the upper microvalve. Because of the connectivity between the two stages, PIN for the next stage is now low. The membrane of the upper microvalve moves away from the valve seat in response to a low value of PIN, causing the upper microvalve to open. At the same time, the low value of PIN, combined with the normally-closed condition of the poppet microvalve, causes the lower valve to close.

The ports supplying the PHI and PLO reference pressures are out of the plane of this cross-section.

The structure may be built from, for instance, fusion-bonded silicon wafers. Alternatively, the plastic-based techniques found most often in microfluidic structures can also be employed [14], provided the material properties and structural dimensions are tailored to achieve the required flow and pressure specifications.

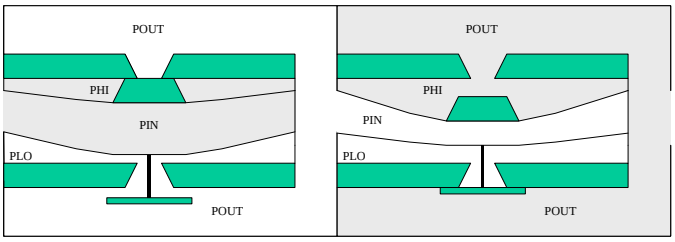

Figure 9: Two cascaded micropneumatic NOR gates (inverters). The upper structure in each inverter is a normally-closed valve, while the lower structure is a normally-closed poppet valve.

TRANSFER CHARACTERISTIC OF A MICRO-PNEUMATIC INVERTER

The quantitative pneumatic flow equations developed earlier in this investigation are easily applied to the micropneumatic NOR gate structure, to analyze its steady-state behavior, and to determine the structural design parameters from the desired performance goals and pressure boundary conditions.

Figure 10 shows just such a representative micropneumatic inverter transfer characteristic. For this calculation, the assumptions used to write Equations (5) were *not* employed. Instead, the full cubic dependence of the mechanical response of the membranes to pneumatic excitation was used. Also, the full expression for the effective flow area of each microvalve was incorporated. The use of these fuller expressions did not affect the results significantly in a quantitative sense, and does not detract at all from the physical nature of Equations (5).

For the design studied in Figure 10, the following parameters are employed: silicon is the structural material; the membrane thickness is 50 μm; the square membrane side length is 4.5 mm; the gas is nitrogen, the gas stagnant temperature is 298 K; the inlet diameter of the upper (normally-closed) valve is 51 μm; inlet diameter of the lower (normally-closed poppet) valve is 85 μm; P_{HI} in the system is 100000 Pa; P_{LO} in the system is 100 Pa; threshold gaps for each device are -2 μm (as before, the minus sign indicates the tension in the membranes which creates the normally-closed condition).

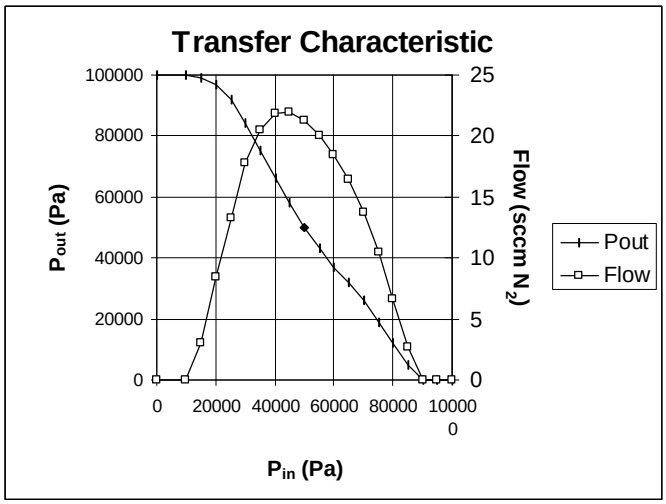

Figure 10: Transfer characteristic for a micropneumatic, fully-complementary inverter or NOR gate.

DISCUSSION

As with their MOSFET counterparts, it is important to note that the pneumatic microvalves reported herein are components for *primary* logic devices. By 'primary', we mean that logic devices based on these components accept an input signal in one form of energy, and deliver an output signal of the same energy form. So, a CMOS inverter accepts an electrical (voltage) input, and delivers an electrical (voltage) output. In the case of micropneumatic logic, a fluidic (pressure) input signal is accepted, and transformed to a fluidic (pressure) output signal. This feature is unlike the microfluidic logic structures reported in the Introduction.

It is worth noting further, that previously reported, pressure-based mass flow controllers, built using a microvalve and a critical orifice [21], are simply a microvalve-flow resistor inverter (analogous to a transistor-resistor logic gate), operated in analog, not digital, mode.

While the micropneumatic logic structures presented apply to compressible fluids (gases), with a small modification they may also be applied successfully to incompressible (liquid) systems, thus enabling microhydraulic logic. This application should be of considerable interest to the microfluidic, bio-MEMS, and μTAS communities, and will be discussed in more detail in a subsequent work.

By further analogy to MOSFET technology, the promise of performance improvements through the reduction in size of micropneumatic logic devices (following the famous microelectronic suggestion of [17]), comes immediately to mind. It will remain for subsequent work to describe the transient response of micropneumatic logic devices, as well as the scaling theory attendant to the relationship between the performance of these devices, and decreases in their size.

Even so, at least one statement concerning speed can be made at this juncture. From the compressible gas flow equations, it is clear that, as with MOSFETs, the saturation velocity (of particles in the control fluid) controls the rate at which information can be transported through the structure. Roughly speaking, for electron flow in silicon, the saturation velocity is 10^7 cm/sec. By comparison, the speed of sound in helium is roughly 10^5 cm/sec. So, we expect the response time for micropneumatic logic gates to be 1% of their comparably sized microelectronic counterparts. While this is certainly slower, it is nonetheless intriguing, especially for applications where electronic processes for information transport and transformation are inappropriate, but some degree of speed is yet beneficial.

CONCLUSIONS

In this work, we have quantified the analogy between microelectronic MOSFETs and pneumatic microvalves, using the flow model we developed previously for compressible gas flow in microvalves. We have applied the model to vertical, 'edgeless' microvalves. The application of the model clarifies several aspects of the microvalve-MOSFET analogy. In particular, it specifies the valve parameters responsible for the threshold pressure P_t. It also identifies the linear MOSFET current equation with subsonic, compressible gas flow, and the saturation MOSFET current equation with sonic, compressible gas flow.

Using this quantification of the analogy, we subsequently devised novel, vertical mode pneumatic microvalve gates, which mimic the behavior of *p*-MOSFET and *n*-MOSFET gates. The analog to the *p*-MOSFET is a normally-closed microvalve, while the analog to the *n*-MOSFET is a normally-closed poppet microvalve.

We combined these two microvalves to realize a complementary, micropneumatic NOR gate, which delivers a logical pressure output signal which is the inversion of an input pressure signal.

Finally, and again by applying the microvalve flow model to this gate structure, we developed the steady-state transfer characteristic for the fully complementary, micropneumatic NOR gate.

REFERENCES

[1] H. Takao, M. Ishida, and K. Sawada, "A pneumatically actuated full in-channel microvalve with MOSFET-like function in fluid channel network." *J. Microelectromech.* **11**(5), pp. 421-426 (2002).

[2] M. J. Zdeblick, "A planar process for an electric-to-fluidic valve." Ph.D. dissertation, Stanford U. (1987).

[3] H. Takao and M. Ishida, "Microfluidic integrated circuits for signal processing using analogous relationship between pneumatic microvalves." *J. Microelectromech.* **12**(4), pp. 497-505 (2003).

[4] M. Minsky, "Virtual Molecular Reality." In Prospects in Nanotechnology: Toward Molecular Manufacturing, pp. 187-195 (M. Krummenacke and J. Lewis, eds., John Wiley & Sons, New York, 1992).

[5] C. Vieider, O. Ohman, and H. Elderstig, "A pneumatically actuated micro valve with a silicone rubber membrane for integration with fluid-handling systems." In *Tech. Dig. 8th IEEE Int'l. Conf. Sol. St. Sens. Act.*, pp. 284–286 (IEEE, Piscataway, NJ, 1995).

[6] D. F. Jensen, *et al*., in *Advances in Fluidics*, pp. 313-338 (F. T. Brown, ed., ASME, New York, 1967).

[7] G. Gunther, "Application of a silicon microvalve to pilot-operation of pneumatic valves." In Recent Advances in Mechatronics (Ed. by O. Kaynak, *et al*., Springer-Verlag, 1999).

[8] K. Hosokawa and R. Maeda, "A pneumatically-actuated three-way microvalve fabricated with polydimethylsiloxane using the membrane transfer technique." *J. Micromech. Microeng.* **10**, pp. 415–420 (2000).

[9] K. Relyea and S. Leng, "Micro-fluidic ring oscillators." WISP Final Project Report, unpublished (Dartmouth College, Hanover, NH, 1995).

[10] _____, "Pneumatic logic devices pushed." *Electronic Design*, p. 4 (Penton Media, Cleveleand, OH, May 24, 1961).

[11] W. Zhan and R. M. Crooks, "Microelectrochemical logic circuits." *J. Amer. Chem. Soc.* **125**, pp. 9934-9935 (2003).

[12] S. K. Cho, *et al.*, "Toward digital microfluidic circuits: creating, transporting, cutting and merging liquid droplets by electrowetting-based actuation." In *Proc. 15th Int'l. Conf. MEMS*, pp. 32-35 (IEEE, Piscataway, NJ, 2002).

[13] R. B. Fair, *et al.*, "Electrowetting-based on-chip sample processing for integrated microfluidics." In *Proc. Int'l. Elec. Dev. Mtg.*, pp. 32.5.1-32.5.4 (IEEE, Piscataway, NJ, 2003).

[14] T. Thorsen, S. J. Maerkl, and S. R. Quake, "Microfluidic large-scale integration." *Science* **298**, pp. 580-584 (2002); M. A. Unger, *et al.*, "Monolithic microfabricated valves and pumps by multilayer soft lithography." *Science* **288**, pp. 113-116 (2000).

[15] T. Vestad, D. W. M. Marr, and T. Munakata, "Flow resistance for microfluidic logic operations." *Appl. Phys. Lett.* **84**(25), pp. 5074-5075 (2004).

[16] W. van der Wijngaart, A. S. Ridgeway, and G. Stemme, "A micromachined knife gate valve for high-flow pressure regulation applications." In *Tech. Dig. 12th IEEE Int'l. Conf. Sol. St. Sens. Act.*, pp. 1931-1934 (IEEE, Piscataway, NJ, 2003).

[17] R. H. Dennard, *et al*., "Design of ion-implanted MOSFETs with very small physical dimensions." *IEEE J. Sol.-St. Circuits* **SC-9,** p. 256 (1974).

[18] A. K. Henning, "Compact pressure- and structure-based gas flow model for microvalves." In *Proceedings, Materials and Device Characterization in Micromachining* (International Society for Optical Engineering, Bellingham, WA, 2000; Y. Vladimirsky and P. J. Coane, eds.), volume 4175, pp. 74-81

[19] A. K. Henning, "Improved gas flow model for microvalves." In *Tech. Dig. 12th IEEE Int'l. Conf. Sol. St. Sens. Act.*, pp. 1550-1553 (IEEE Press, Piscataway, NJ, 2003).

[20] M. DiGiovanni, Flat and Corrugated Diaphragm Design Handbook. (Marcel Dekker, New York, 1989).

[21] A. K. Henning, *et al*., "Microfluidic MEMS for semiconductor processing." *IEEE Trans. Comp. Pkg. Mfg. Tech.* **21**(4), pp. 329-337 (1998).

[22] W. van der Wijngaart, "A study of orifice-controlled flow for microvalve design optimization." (In *Designing Microfluidic Control Components*, Ph.D. Dissertation, Paper #8, Royal Institute of Technology, Stockholm, Sweden, 2002).